PREDICTION OF THE CRIPPLING LOAD OF OMEGA-STRINGER STIFFENED COMPOSITE SHELLS

M. Quatmann[1*], M. Chaves Vargas[1], M. A. Lakshmanan[1] and H.-G. Reimerdes[1]

[1]*Institut für Leichtbau, RWTH Aachen University, Wüllnerstraße 7, 52062 Aachen*
**quatmann@ilb.rwth-aachen.de*

Keywords: rapid sizing method, crippling load calculation, stringer-stiffened shells.

Abstract
In order to rapidly and efficiently design composite stiffened structures, computationally efficient methods are still of significant importance. In this regard, an analytically based rapid sizing method for the crippling load computation of composite stringers and stringer-stiffened shells is proposed. Here, the focus is on the behaviour of stiffeners with closed cross-sections widely referred to as omega-stringers. The crippling load is the ultimate load short stiffeners and stiffened shells can resist before final failure. Usually, both shell and stiffener start to buckle locally before final failure and a load redistribution from the center of the buckles towards the remaining straight edges occurs. As soon as the crippling load is reached composite stringers instantly fail due to fibre-fracture ongoing with a significant drop-down of the load within the load-displacement curve. Based on an analytical description of the buckling and postbuckling behaviour, a fast calculation method for the crippling load of composite stringers and stiffened shells is derived. Here, following the stress distribution calculation in the postbuckled state, a fibre-fracture criterion is used to determine the crippling load of composite stiffened shells. The results obtained using the proposed rapid sizing method are compared to shell-based finite element model computations as well as available test data and results have generally been found in good agreement.

1 Introduction
The crippling load is the ultimate load a stiffener loaded in uniaxial compression can carry before final failure occurs. Because long stiffeners usually fail by buckling before the crippling load is reached, the load can experimentally and numerically only be determined if the stiffener is sufficiently short. The crippling load of composite stringers with different stacking sequences has been intensively studied by Spier [1-4]. Additionally, the crippling phenomenon has been further studied numerically by Kweon [5] as well as experimentally by Bonanni [6]. Here, the crippling load is computed based on an analytical approach for the postbuckling behaviour of an axially loaded long plate simply supported at all edges. Once the postbuckling stress distribution is known the proposed computation method for crippling first computes the critical area where fibre fracture occurs first. Afterwards, the critical load at this stage, the crippling load, is computed.

2 Analytical computation of crippling loads

The key problem that needs to be solved in order to predict the crippling load with adequate precision is the computation of buckling load and postbuckling stiffness as well as postbuckling load redistribution of a long rectangular plate loaded in axial compression. The buckling loads of orthotropic flat plate stripes with all edges simply supported or three edges simply supported and one edge free (the two most important components of stiffener sections) are well known [7] and the derivation of the formulas will not be shown here. Here, the postbuckling stress distribution and stiffness will be computed for an orthotropic plate with all edges simply supported. In contrast to many publications in this field that mainly study skin buckling and therefore assume the unloaded edges straight, edges are assumed to be free to pull in as shown in Figure 1.

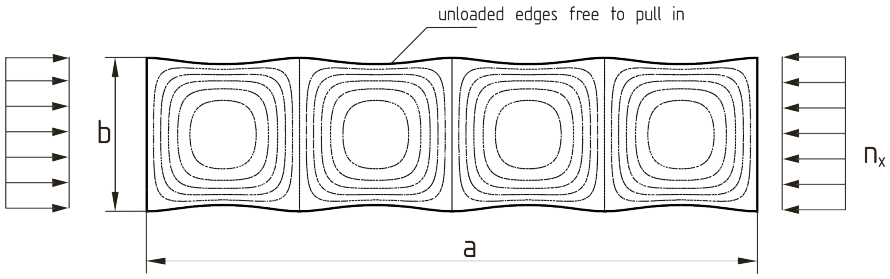

Figure 1. Simply supported rectangular plate loaded in compression with unloaded edges free to pull in

The membrane strains including couplings to out-of-plane displacements are (see e.g. [8]):

$$\epsilon_x = u_{,x} + \frac{1}{2}{w_{,x}}^2 \; ; \; \epsilon_y = u_{,y} + \frac{1}{2}{w_{,y}}^2 \; ; \; \gamma_{xy} = u_{,y} + v_{,x} + w_{,x}w_{,y} \tag{1}$$

Additionally the curvatures are (see e.g. [8]):

$$\kappa_x = -w_{,x,x} \; ; \; \kappa_y = -w_{,y,y} \; ; \; \kappa_{xy} = -2w_{,x,y} \tag{2}$$

As already initially stated, the computations are performed for orthotropic material properties. In this regard, force flows and moment flows are connected to strains and curvatures as follows:

$$\begin{pmatrix} \epsilon_x \\ \epsilon_y \\ \gamma_{xy} \\ m_x \\ m_y \\ m_{xy} \end{pmatrix} = \begin{bmatrix} a_{11} & a_{12} & 0 & 0 & 0 & 0 \\ a_{12} & a_{22} & 0 & 0 & 0 & 0 \\ 0 & 0 & a_{66} & 0 & 0 & 0 \\ 0 & 0 & 0 & d_{11} & d_{12} & 0 \\ 0 & 0 & 0 & d_{12} & d_{22} & 0 \\ 0 & 0 & 0 & 0 & 0 & d_{66} \end{bmatrix} \cdot \begin{pmatrix} n_x \\ n_y \\ n_{xy} \\ \kappa_x \\ \kappa_y \\ \kappa_{xy} \end{pmatrix} \tag{3}$$

Now, the potential can be created by summing up membrane energy and bending energy:

$$\Pi = \Pi_1 + \Pi_2 \tag{4}$$

with:

$$\begin{aligned} \Pi_1 &= \frac{1}{2}\int_A n_x\epsilon_x + n_y\epsilon_y + n_{xy}\gamma_{xy}\,dA \\ \Pi_2 &= \frac{1}{2}\int_A m_x\kappa_x + m_y\kappa_y + m_{xy}\kappa_{xy}\,dA \end{aligned} \tag{5}$$

Finally, the potential is only a function of the three displacement functions u, v, w. The approximation functions for u, v and w are chosen as proposed by Cox [9] for the given boundary conditions. The out-of-plane displacement is not influenced by the boundary conditions at the unloaded edge and results to:

$$w = w_{11}\sin\left(\frac{\pi x}{a}\right)\sin\left(\frac{\pi y}{b}\right) \tag{6}$$

However, for the inplane displacements u and v, the displacements at the unloaded edges need to be taken into consideration. In this regard, Cox [9] formulated the following displacement functions:

$$u = \frac{a}{2\pi}\sin\left(\frac{2\pi x}{a}\right)\left[u_0 + \sum_{i=1}^{\infty} u_i\cos\left(2\frac{\pi y i}{b}\right)\right] - x\epsilon_{xm} \tag{7}$$

$$\begin{aligned} v &= \frac{b}{2\pi}\left[\left(X\cos\left(\frac{2\pi x}{a}\right) - \epsilon_{ym}\right)\left(\frac{2\pi\, y}{b} - \pi\right)\right. \\ &+ \left.\sum_{i=1}^{\infty}\left(V_{Si} + V_i\cos\left(\frac{2\pi x}{a}\right)\right)\sin\left(\frac{2\pi y i}{b}\right)\right] \end{aligned} \tag{8}$$

The insertion of the proposed approximation functions for the displacements u, v and w into the potential and a subsequent minimization with respect to all unknown variables leads to a closed form solution for all unknowns. Once all variables have been computed the postbuckling force flow can be obtained. Here, the infinite row has been computed with a maximum of ten contributors. The equations remain solvable analytically even if the maximum number of terms in the row is increased further but also the complexity of the obtained results increases. However, taking only the most important terms into account (the first ones) leads to the following approximation for the effective stiffness after buckling, $a_{11,eff}$, of a plate loaded in axial direction with the unloaded edges free to pull in.

$$\frac{a_{11,eff}}{a_{11}} = \frac{q_1 + q_2 + q_3}{q_1 + 2q_2 + 3q_3} + \frac{1}{k}\left(1 - \frac{q_1 + q_2 + q_3}{q_1 + 2q_2 + 3q_3}\right) \tag{9}$$

with:

$$\begin{aligned} q_1 &= \left((\xi + 1 + 2\,\zeta)\,\pi^2 - 6 - 12\,\zeta\right) \\ q_2 &= 2\,\left(\pi^2 - 6\right)\mu \\ q_3 &= 3\,(\xi + 1 + 2\,\zeta)\,\xi\,\mu^2 + \left(3\,\xi + \xi\,\pi^2 + 2\,\pi^2\zeta - 12\,\zeta\right)\mu + \pi^2 - 6 \end{aligned} \tag{10}$$

Here, μ, ξ and ζ are defined as follows:

$$\begin{aligned} \mu &= \frac{a_{11}d_{11}}{a_{22}d_{22}} \\ \xi &= \frac{a_{66}}{a_{11}}\sqrt{\frac{d_{22}}{d_{11}}} \\ \zeta &= \frac{a_{12}}{a_{11}}\sqrt{\frac{d_{22}}{d_{11}}} \end{aligned} \tag{11}$$

Using this comparatively simple approximation functions the initial postbuckling stiffness could be computed with an accuracy of approximately 8% for several tested laminates when compared to higher order approximations. For example, for an isotropic plate the initial postbuckling stiffness is computed to 43% of the initial stiffness whereas the converged result is 41% [9].

3 Validation and numerical verification for a square tube

In order to analyze real structures, stiffeners are decomposed into plate assemblies as shown in Figure 2. Then, for each individual plate with boundary conditions as shown in Figure 1, the effective postbuckling stiffness as well as the critical fibre fracture strain are computed.

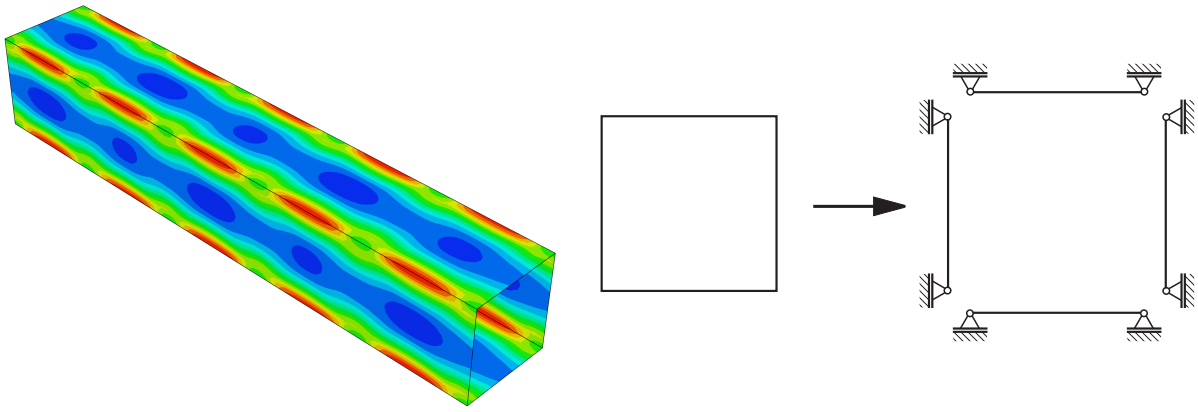

Figure 2. Structural idealization of square tube cross-section for use in analytical method

The axial stress varies at the edges along the length of the tube or corresponding plate. As the specimens will fail at the peak stress areas, these peak stresses need to be computed in addition to the postbuckling stiffness. Especially if 0°-plies, which are usually most critical with regard to first fibre fracture, are not directly in the middle of the plate, curvatures can significantly increase the stress in these plies. The highest curvatures are present in the middle of the buckles and decrease to zero directly at the edges. Therefore, directly after buckling the peak stress occurs at the center of the buckle as shown in Figure 3. When the load further

exceeds the buckling load the point of peak stress continously moves from the center of the buckle towards the edges. In most laminates the peak stress occurs at the edges when the present load exceeds the buckling load three times.

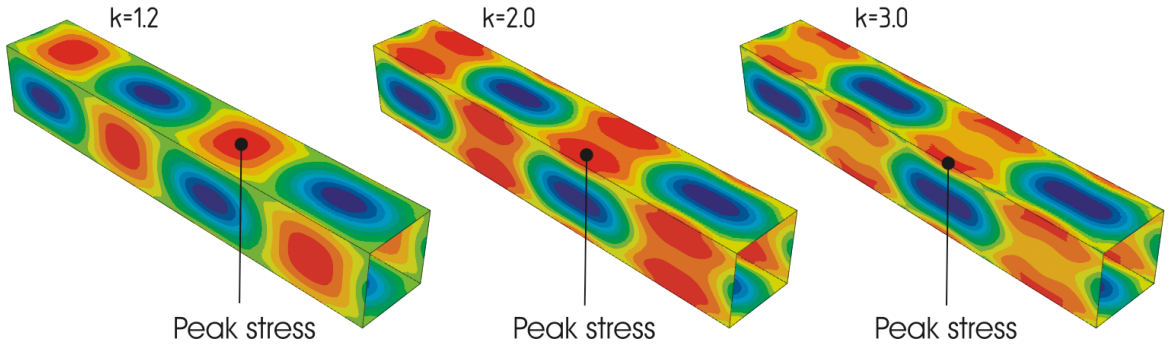

Figure 3. Peak stress at edges of square tube when buckling load is k-times exceeded

In order to validate the presented rapid sizing method, crippling load computations have been performed for a T300/Epoxy laminate as described in [1] and results are plotted non-dimensionlized as proposed by Spier [1]. Additionally, test results from [1] obtained from square tube tests have been included into Figure 4. Figure 4 also shows the influence of imperfections on the critical crippling load.

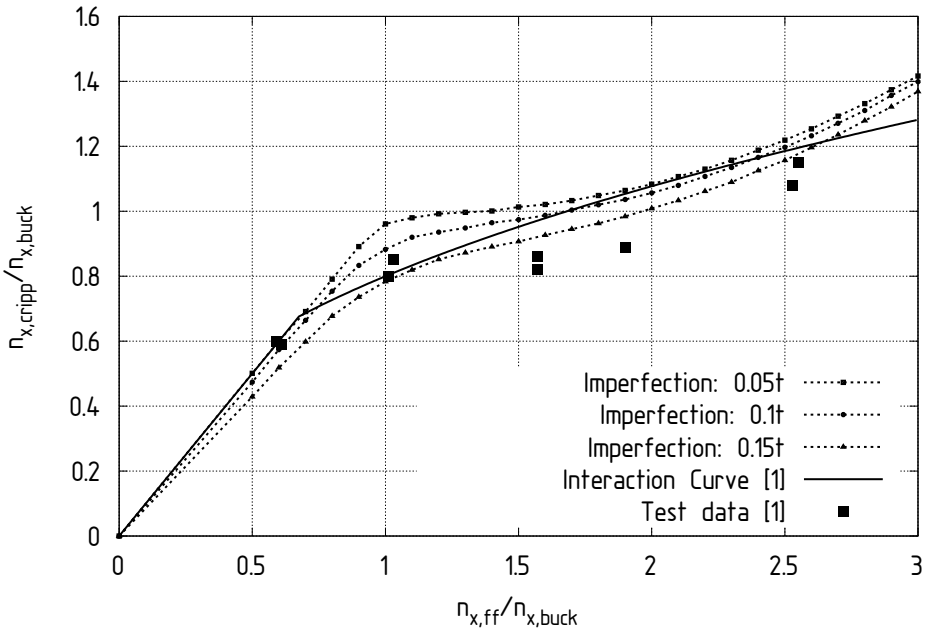

Figure 4. Non-dimensional crippling curves including empirical curves from Spier

As can be seen the analytically derived non-dimensional crippling curves are, especially taking into consideration the approximate nature of the computation, in good agreement with the experimental data.

5 Conclusion and outlook

A fast analytical method for the approximation of the crippling load of composite stringers and omega-type stringer stiffened shells has been proposed. The method is based on the

decomposition of arbitrary stiffener profiles into individual plates. Here, no interaction between the different plates is taken into consideration. For the individual plates the computation of the postbuckling behaviour of a simply supported plate with the unloaded edges free to pull in is performed. Crippling failure is defined as first occurance of critical strain taking into consideration the postbuckling stress distribution. The method has been compared to numerical as well as experimental results and generally a good agreement has been found.

References

[1] Spier, E.E. Stability of Graphite/Epoxy Structures with Arbitrary Symmetrical Laminates, *Experimental Mechanics,* **18(11)**, pp. 401-408 (1978).

[2] Spier, E.E., Klouman, F.L. *Empirical Crippling Analysis of Graphit/Epoxy Laminated Plates* in "Proceedings of *Composite Materials: Testing and Design (4th Conf.)"*, ASTM STP 617 (1977).

[3] Spier, E.E., Klouman, F.L. *Ultimate Compressive Strength and Nonlinear Stress-Strain Curves of Graphite/Epoxy Laminates* in "Proceedings of *8th SAMPE Conf., "Bicentennial of Materials Progress – Part II"*, Seattle, WA (1976).

[4] Spier, E.E. *Crippling/Column Buckling Analysis and Test of Graphite/Epoxy-stiffened Panels* in "Proceedings of *AIAA/ASME/SAE 16th Structures, Structural Dynamics and Materials Conf. th SAMPE Conf.*, Denver, CO (1975).

[5] Kweon, J.-H. Crippling analysis of composite stringers based on complete unloading method, *Computers and Structures,* **80**, pp. 2167-2175 (2002).

[6] Bonanni D.L., Johnson E.R., Starnes J. Local crippling of thin-walled graphite-epoxy stiffeners. AIAA Journal, **29(11)**, pp. 1951-1959 (1991).

[7] Structures and Mechanisms Division at ESA/ESTEC, *Composite Design Handbook for space structure applications*, ESA PSS-03-1101 Issue 1 (1986).

[8] Jones, R.M., *Mechanics of Composite Materials.* New York, Hemisphere Publ. (1975).

[9] Cox, H.L., *The Buckling of Plates and Shells.* Oxford, Pergamon Press (1963).